Sum-Rule Constraints on the Surface State Conductance of Topological Insulators

K. W. Post,[1,*] B. C. Chapler,[1] M. K. Liu,[1] J. S. Wu,[1] H. T. Stinson,[1] M. D. Goldflam,[1] A. R. Richardella,[2] J. S. Lee,[2] A. A. Reijnders,[3] K. S. Burch,[4] M. M. Fogler,[1] N. Samarth,[2] and D. N. Basov[1]

[1]*Physics Department, University of California-San Diego, La Jolla, California 92093, USA*

[2]*Department of Physics, The Pennsylvania State University, University Park, Pennsylvania 16802, USA*

[3]*Department of Physics & Institute for Optical Sciences, University of Toronto, Toronto, Ontario M5S 1A7, Canada*

[4]*Department of Physics, Boston College, Chestnut Hill, Massachusetts 02467, USA*

(Received 3 June 2014; revised manuscript received 5 July 2015; published 11 September 2015)

We report the Drude oscillator strength D and the magnitude of the bulk band gap E_g of the epitaxially grown, topological insulator $(\mathrm{Bi,Sb})_2\mathrm{Te}_3$. The magnitude of E_g, in conjunction with the model independent f-sum rule, allows us to establish an upper bound for the magnitude of D expected in a typical Dirac-like system composed of linear bands. The experimentally observed D is found to be at or below this theoretical upper bound, demonstrating the effectiveness of alloying in eliminating bulk charge carriers. Moreover, direct comparison of the measured D to magnetoresistance measurements of the same sample supports assignment of the observed low-energy conduction to topological surface states.

DOI: 10.1103/PhysRevLett.115.116804 PACS numbers: 73.50.-h, 73.25.+i, 78.30.-j

The prediction and discovery of Dirac-like gapless surface states (SSs) (see Fig. 1) at the interface between a topological insulator (TI) and a trivial insulator have vaulted TIs to the vanguard of condensed matter physics [1]. Surface probes such as angle resolved photoemission spectroscopy and scanning tunneling spectroscopy have been extremely successful in verifying and discovering novel phenomena associated with the SSs (e.g., Refs. [2–5]). However, progress in the field has been plagued by native defects, resulting in significant concentrations of bulk charge carriers. These bulk dopants inhibit isolation and utilization of SS phenomena [6]. In order to realize many of the novel scientific and technological advances that could blossom from the unique electronic, spin, and optical properties of SSs in TIs, it is paramount to eliminate the bulk dopants.

Two archetypal strong TIs (topological invariant $\nu_0 = 1$ [1]) that are known to suffer from materials issues related to bulk dopants are $\mathrm{Bi_2Te_3}$ and $\mathrm{Sb_2Te_3}$. However, epitaxial films of $\mathrm{Bi_2Te_3}$ can be n-type bulk conductors [6,7], whereas $\mathrm{Sb_2Te_3}$ films are p-type bulk conductors [8]. Based on this observation, TI materials have been grown where the ratio Bi:Sb in $(\mathrm{Bi,Sb})_2\mathrm{Te}_3$ (BST) is tuned to produce a compensated material with bulk insulating properties [9–11]. Here, we prove, using optical spectroscopy, the acute effectiveness of alloying in reducing or eliminating bulk charge carriers. The advantage of our optical experiments is that they give direct access to the frequency dependent electrodynamic response of free carriers in a metal via the Drude peak. In our $(\mathrm{Bi,Sb})_2\mathrm{Te}_3$ film we find the Drude oscillator strength D sufficiently low as to lie at or below the upper bound that is theoretically anticipated for an isolated Dirac SS Drude response (i.e., a Drude response with no bulk contribution) (see Table I). These infrared data are complemented by the charge carrier density n and mobility μ from Hall effect measurements, as well as the magnetoresistance, which are all consistent with low-energy conduction arising from the topological SS.

We begin by describing the optical response of Dirac electrons in a strong TI, neglecting potential interband bulk → SS transitions (or vice versa) [15]. The simplest Dirac electron system is composed of linear bands (LB), without spin or valley degeneracy, where the dispersion is given by $E(k) = kv_F$, as illustrated schematically in Figs. 1(a) and 1(b). In this system, the total conductance $G_{\mathrm{tot}}^{\mathrm{LB}}$ is the sum of an intraband $G_{\mathrm{intra}}^{\mathrm{LB}}(\omega)$ and an interband $G_{\mathrm{inter}}^{\mathrm{LB}}(\omega)$ component. When the Fermi energy E_F is at the Dirac point, theory predicts that SS interband transitions give rise to a frequency independent conductance of $G_{\mathrm{inter}}^{\mathrm{LB}} = \frac{1}{8}(\pi e^2/h)$ [16]. However, the area of the Fermi surface is zero, yielding $G_{\mathrm{intra}}^{\mathrm{LB}} = 0$. When E_F is shifted away from the Dirac point, empty states suppress interband transitions at energies below $2|E_F|$, as illustrated in Fig. 1(b), resulting in $G_{\mathrm{inter}}^{\mathrm{LB}}(\omega) = 0$ for $\omega < 2|E_F|$. Importantly, the f-sum rule [17] demands that the total spectral weight of the Dirac electrons $\int_0^\infty G_{\mathrm{tot}}^{\mathrm{LB}} d\omega$ be conserved [18,19]. Therefore, the loss of spectral weight in $G_{\mathrm{inter}}^{\mathrm{LB}}(\omega)$ must be compensated by a gain in $G_{\mathrm{intra}}^{\mathrm{LB}}(\omega)$, leading to

$$G_{\mathrm{inter}}^{\mathrm{LB}} 2|E_F| = \int_0^\infty G_{\mathrm{intra}}^{\mathrm{LB}} \hbar d\omega. \quad (1)$$

It is customary to express the relationship between intraband spectral weight and Drude oscillator strength D_{LB}^s as

$$\int_0^\infty G_{\mathrm{intra,LB}}(\omega) \hbar d\omega = \frac{\pi}{30\Omega} D_{\mathrm{LB}}^s, \quad (2)$$

which implies the simple relationship between E_F and D_{LB}^s

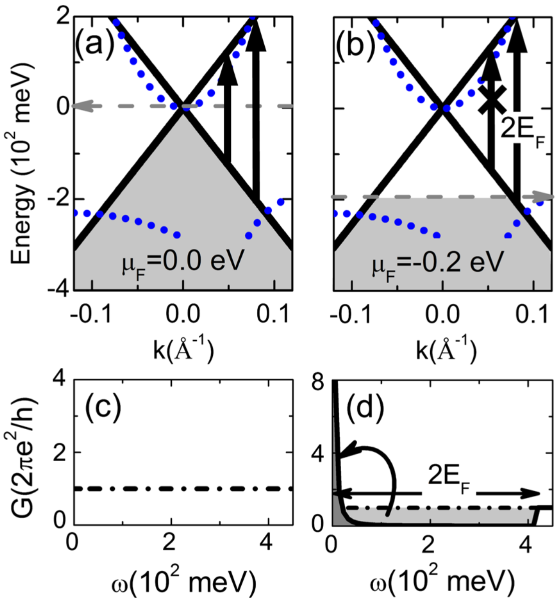

FIG. 1 (color online). Panels (a) and (b) show the band structure of a model TI, where the SS is composed of simple linear bands. The bulk band structure is also indicated by the dotted blue lines, consisting of two hole bands and an electron band. In (a) E_F is at the Dirac point, while in (b) E_F is 0.20 eV below the Dirac point, where the arrows in both panels schematically show the allowed transitions. In (a), interband transitions are allowed at all energies, giving rise to the conductance spectra shown in (c). When E_F is shifted below the Dirac point, transitions cannot occur from the depopulated region. Thus, transitions are suppressed below $2|E_F|$, giving rise to the conductance spectra shown in (d).

$$D^s_{\mathrm{LB}} = \frac{60\Omega}{\pi} G^{\mathrm{LB}}_{\mathrm{inter}} |E_F|. \quad (3)$$

The conductivity of the TI is dominated by the surface states, provided E_F is located outside of the bulk bands. It is customary to measure E_F relative to the Dirac point. Then, for p-type conductivity, E_F, defined relative to the Dirac point, cannot lie within the bulk bands. Therefore, for p-type (n-type) SS conduction, the maximum value of D^s_{LB}, occurs when the Dirac point is at the conduction band minimum (valence band maximum), and E_F is at the valence band maximum (conduction band minimum). Then, the energy that corresponds to the maximum value of E_F is simply E_g, with the maximum value of D^s_{LB}, $D^s_{\mathrm{LB,max}}$, given by $D^s_{\mathrm{LB,max}} = (N_S)(60\Omega/\pi)G_{\mathrm{TI}}E_g$, where N_S is the number of probed interfaces between systems with different topological indices. Here, $N_S = 2$ since optical transmission probes two topological surfaces, i.e., the interface between the film and the vacuum, and that between the film and the substrate.

The straightforward relationship between D_{LB} and E_F in Eq. (3) is useful for estimating the Drude spectral weight that could arise from SSs, and for intuitively understanding the spectral weight transfer in TI systems. Importantly, the resilience of the f-sum rule to external parameters has been experimentally verified numerous times in a prototypical surface state conductor: graphene. Even with gating, where additional charge carriers are introduced, the f-sum rule is found to be correct within the experimental error bars [20]. The reason for this is that the dominant effect of gating is a redistribution of spectral weight, while the increase in carriers is a relatively small perturbation. Importantly, TI materials are often not well modeled by linear bands. Instead, significant hexagonal warping effects are observed in Bi_2Te_3 and $(Bi, Sb)_2Te_3$ as well as asymmetry between the upper and lower portions of the Dirac cone [4,9]. These combined effects modify the conductance from the constant value shown in Fig. 1(c), and therefore change the value of D^s for a given E_F [16]. To more accurately estimate $D^s_{\max}$, we have considered the optical response of a more realistic SS dispersion of a similarly doped sample [9,16]. This additional analysis suggests that $D^s_{\max}$ could be enhanced by approximately 25%, depending on the sample in question [21].

TABLE I. Bulk band gap E_g, experimental Drude oscillator strength D from transmission based experiments, modeled Drude oscillator strength D^s_{3layer} where the conductance is assumed to be from two topological surfaces with an insulating bulk, and theoretical upper bound of the free Dirac SS Drude oscillator strength $D^s_{\mathrm{LB,max}}$ of prototypical strong TIs obtained using the bulk energy gap, and assuming bands with linear dispersion. Values of D are all taken from low-temperature data (6–20 K). All units are in meV.

TI material	E_g	D	D^s_{3layer}	$D^s_{\mathrm{LB,max}}$	References
Bi_2Se_3	300	0.5–0.70	⋯	0.17	[2,12]
Bi_2Te_3	142	1.26	⋯	0.08	[7]
$Bi_{1.5}Sb_{0.5}Te_{1.8}Se_{1.2}$	340	1.42	⋯	0.20	[13]
Bi_2Te_2Se[a]	290	⋯	0.83	0.08	[10]
$Bi_{0.92}Sb_{1.08}Te_3$	207	0.13	0.14	0.12	This work
Bi_2Se_3	300	0.09	⋯	0.17	[14]

[a]The results of Ref. [10] are from reflection based experiments, and thus only one topological surface is considered.

In light of the constraints on D imposed by the f-sum rules, we experimentally determined D and E_g of $(Bi, Sb)_2Te_3$ through a combination of terahertz time-domain spectroscopy and Fourier transform infrared spectroscopy (FTIR). Details of the sample growth and experimental techniques are included in Ref. [21]. In Fig. 2(a), we plot the frequency dependent conductance spectra $G(\omega)$ [real part of $\tilde{\sigma}(\omega) \times$ thickness] of our $(Bi, Sb)_2Te_3$ film from 2–18 meV, the relevant energy scale for the Drude response. The most prominent feature at all temperatures is the narrow resonance centered near 6 meV, which is attributed to a phonon. There is another, weaker phonon resonance, slightly higher in energy, at roughly 8 meV. The assignment of these phonon modes is discussed in Ref. [21] At energies below these features, we observe a relatively flat but finite $G(\omega)$ related to the Drude response.

To quantify the Drude oscillator strength D, we construct a Drude-Lorentz model to describe the conductance of the BST system:

$$G(\omega) = \frac{1}{15\Omega} \frac{D\tau}{1 + (\omega\tau)^2} + \sum_{j=1}^{n} \frac{A_j \Gamma_j \omega^2}{(\omega^2 - \omega_{0j}^2)^2 + (\Gamma_j \omega)^2}, \quad (4)$$

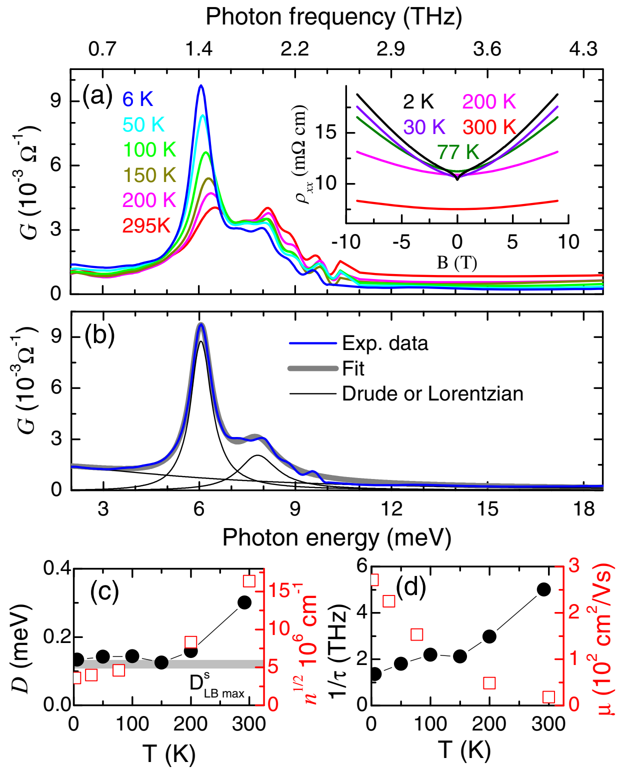

FIG. 2 (color online). (a) Temperature dependent spectrum of the conductance of $(\mathrm{Bi,Sb})_2\mathrm{Te}_3$ obtained from terahertz time-domain spectroscopy and FTIR. The inset shows (symmetrized) dc magnetoresistivity data for this film. The "cusp" at the low-B field in the 2 K data is indicative of weak antilocalization. (b) Drude-Lorentz model fit (4) (gray) of the 6 K experimental conductance (blue). Individual Drude or Lorentzian oscillators are displayed as thin black lines. (c) Temperature dependence of the Drude oscillator strength D (black points) corresponding to the left axis, and square root of the charge carrier density n (open red squares) extracted from Hall effect measurements, corresponding to the right axis. The upper bounds for the Drude response of the linear SS ($D^s_{\mathrm{LB,max}} \pm 10\%$), and more realistic estimate of the SS contribution including hexagonal warping ($D^s_{\mathrm{BST,max}}$) in $(\mathrm{Bi,Sb})_2\mathrm{Te}_3$, are indicated by the light gray and dark gray bars, respectively. (d) Temperature dependence of the free carrier scattering rate $1/\tau$ from optics (black points, left axis) and charge mobility μ from Hall effect measurements (open red squares, right axis).

where the first term describes the Drude response and the second term corresponds to Lorentzian resonances with amplitude A, width Γ, and center frequency ω_0. A representative Drude-Lorentz model fit is shown in Fig. 2(b) for the 6 K spectrum. The Drude-Lorentz models and the corresponding data at higher temperatures are shown in Ref. [21]. To independently confirm the values of D obtained from the model, we also considered a multilayer model where the BST system consisted of two conducting surface layers and an insulating bulk [21]. The Drude oscillator strength attributed to these conducting surface layers was consistent with the value of D extracted from the measured $G(\omega)$ spectra.

Above 150 K, both D and $1/\tau$ for $(\mathrm{Bi,Sb})_2\mathrm{Te}_3$ [black points in Figs. 2(c) and 2(d)] decrease as temperature is reduced. Since $D \propto \sqrt{n}$, for 2D Dirac states, the reduction in D indicates a reduction in charge carriers, consistent with thermal activation at higher temperatures.The charge carrier density n extracted from Hall effect measurements on this film indicates p-type conduction, as is typical of $(\mathrm{Bi}_{1-x}\mathrm{Sb}_x)_2\mathrm{Te}_3$ systems [9,11], with thermal activation at $T > 150$ K [open red squares in Fig. 2(c)]. Moreover, the magnetoresistance data at 200 and 300 K, shown in the inset to Fig. 2(a), show a nonlinear trend with magnetic field B, suggesting multiband transport, also consistent with the notion of thermally activated bulk states coexisting with SSs. Furthermore, since thermally activated charge carriers are not topologically protected, it is likely that their presence would yield a lower mobility (larger $1/\tau$). Therefore, the simultaneous decrease in D and $1/\tau$ as the temperature is lowered, supports the notion that thermally activated charge carriers are frozen out, leaving only high mobility carriers. The Hall parameters n and μ for these high temperature data in Fig. 2 were fit only in the linear regime (-1 T $< B <$ 1 T).

Below 150 K, D and $1/\tau$ remain relatively constant near 0.13 meV and 2 THz, respectively. Importantly, our low temperature D value lies right at the threshold of $D^s_{\mathrm{LB,max}} \pm 10\%$ for $(\mathrm{Bi,Sb})_2\mathrm{Te}_3$, indicated by the light gray bar in Fig. 2(c). This latter fact indicates that the measured Drude spectral weight is consistent with a SS dominated response. Moreover, the low temperature value of D is roughly 5 to 10 times lower than most of those previously reported for other representative TIs (see Table I), with the exception of a recent report for Cu-doped $\mathrm{Bi}_2\mathrm{Se}_3$ [14]. The next lowest experimentally measured D come from $\mathrm{Bi}_2\mathrm{Se}_3$ [12], in which the D values suggest E_F is in the bulk conduction band. However, in this latter case, corrections to the $\mathrm{Bi}_2\mathrm{Se}_3$ SS band structure mentioned earlier [12] and the persistence of 2D topological SSs to well above the conduction band minimum [35] do imply that D is consistent with a significant SS transport component in $\mathrm{Bi}_2\mathrm{Se}_3$.

To verify that the measured parameters $D^{\mathrm{exp}} = 0.13$ meV and $n^{\mathrm{exp}}_{\mathrm{2D}} = 1.3 \times 10^{13}$ cm^{-2} are consistent with surface dominated transport, we can compare our results to that expected from experimentally obtained SS dispersion of TI materials with a similar $(\mathrm{Bi,Sb})_2\mathrm{Te}_3$ composition [9,11]. For this comparison we will utilize Eq. (3) and the relationship between E_F and the carrier density of a single surface (n_{SS}) [20]

$$E_F = \hbar v_0 \sqrt{4\pi n_{\mathrm{SS}}} \tag{5}$$

to directly relate E_F, n_{SS}, and D via

$$D^s_{\mathrm{LB}} = (N_s)\frac{60\Omega}{\pi} G_{\mathrm{TI}} \hbar v_0 \sqrt{4\pi n_{\mathrm{SS}}}. \tag{6}$$

For direct comparison between transport and optics, we use $n_{\mathrm{SS}} = n^{\mathrm{exp}}_{\mathrm{2D}}/2$, assuming the carriers were divided between two surfaces and $v_0 = 3.8 \times 10^5$ m/s, consistent with both photoemission and transport measurements of p-type SS carriers [11,36]. These values yield $D^s_{\mathrm{LB}} = 0.13$ meV, exactly reproducing our measured value. Moreover, this analysis corresponds to $E_F = 0.22$ eV, in close agreement with the measured E_G of 0.206 eV, suggesting the optical response is close to the constraints imposed by the sum rule analysis. If the additional contribution to D from the bulk bands is taken into account, in the regime where $E_F \approx E_G$, we recover our experimentally measured value of D when $E_F = 0.211$ eV. This analysis, which is detailed in Ref. [21], suggests E_F penetrates only up to 5 meV into the bulk bands, and bulk carriers constitute only 2% of the total $n_{2\mathrm{D}}$. Hexagonal warping, and other modifications to the SS dispersion, discussed more in Ref. [21], suggest that even smaller values of E_F, where $E_F < E_G$, may reproduce the measured D and $n^{\mathrm{exp}}_{2\mathrm{D}}$ values. Alternatively, we considered the case that the optical response arises from the bulk valence bands. Prior work has shown that the bulk valence band structure in the $(\mathrm{Bi,Sb})_2\mathrm{Te}_3$ system consists of a light hole band (LHB) and heavy hole band (HHB) [3,37,38]. The effective masses of the LHB and the HHB are $0.11m_e$ and $1.0m_e$ respectively, and the top of the HHB is approximately 30 meV below the LHB [37,38]. To recover the correct value of D for this sample, E_F would be 30 meV below the top of the LHB, However, this would yield an $n_{2\mathrm{D}}$ of $5 \times 10^{12}\ \mathrm{cm}^{-2}$, over a factor of 2 smaller than what was measured.

Prior experiments have also pointed out that conventional SSs may coexist with the topologically protected SS of a TI [35]. Typically, the conventional SSs appear as a result of band bending, and are close in energy to the bulk bands, and contribute to the conductivity when $E_F \approx E_G$. Therefore, the large magnitude E_F required to access the conventional SSs, combined with their additional metallic response, would likely push D well above the limit imposed by f-sum rule analysis. It is therefore unlikely that our measured response has a significant component from the conventional SSs.

Further evidence of a dominant topological SS contribution to the response of the $(\mathrm{Bi,Sb})_2\mathrm{Te}_3$ system is identified in magnetoresistance measurements, plotted in the inset to Fig. 2. At low temperature, the magnetoresistance data show linear behavior with B, indicative of single band transport. Moreover, the figure reveals weak antilocalization in (symmetrized) magnetoresistance measurements (i.e., the cusp at the low-B field in the 2 K data), which has been thought to be a hallmark signature of topological SS transport [39]. However, theoretical work has shown that antilocalization may occur even in systems with bulk dominated transport, and therefore, antilocalization by itself, cannot be considered conclusive evidence for surface states [40]. Despite this stipulation, the magnetoresistance data, in conjunction with the low value of D revealed from optics, are consistent with low temperature transport that is dominated by topologically protected SSs.

The picture that emerges from the comparison of transport, optics, and previously measured photoemission is that the Dirac point is near the bottom of the conduction band, with E_F near the top of the valence band, as is illustrated in Fig. 1(b). Likewise, we illustrate the bulk band structure consisting of two hole bands offset from the Γ point, with an electron band at the Γ point, as measured previously [9,11,38]. The relative positioning of E_F, the Dirac point, and bulk bands that we propose has been observed in similar, albeit more highly doped, $(\mathrm{Bi}_{1-x}\mathrm{Sb}_x)_2\mathrm{Te}_3$ thin films [11]. Indeed, the distance from the Dirac point to the top of the valence band, as well as v_0 in this latter work, is consistent with our measurements. It is important to note that photoemission measurements of similarly doped samples often show that the Dirac point is below E_F [9], in contrast to our measurement of p-type carriers. This discrepancy can be understood in light of the aging effects, often observed TI systems, which generally shift the Dirac point downward relative to E_F. It is then likely that the capping layer of Se prevents the band bending, and the resulting accumulation layers, observed in other samples [35,36], yielding a response dominated by p-type SS carriers. Unfortunately, this same capping layer prevents direct verification of this hypothesis in our particular sample via photoemission.

The totality of our data clearly show that $(\mathrm{Bi,Sb})_2\mathrm{Te}_3$ alloys are a promising vehicle for advancing the field of TIs. In particular, the Drude oscillator strength lies at the threshold of the SS response upper bound, demonstrating the effectiveness of the alloy in reducing or eliminating bulk charge carriers. Furthermore, comparison of Drude parameters from optics to transport parameters from the Hall effect, coupled with weak antilocalization observed in low-temperature magnetotransport, shows consistency with surface transport with $v_0 \sim 4 \times 10^5$ m/s, in accord with angle resolved photoemission spectroscopy results [11]. Therefore, our data imply that $(\mathrm{Bi,Sb})_2\mathrm{Te}_3$ is an optimal candidate for isolating SS properties in further studies of keen interest, such as magneto-optical measurements [41–43] and electrostatic modification of SS charge carrier density in electric field effect devices [44–46].

Sample growth and characterization at Penn State was supported by DARPA (Grant No. N66001-11-1-4110), ONR (Grant No. N00014-12-1-0117), and ARO-MURI (Grants No. W911NF-12-1-0461) and No. ECS-0335765). Work at the University of California, San Diego (UCSD), on optical phenomena in vdW materials is supported by DOE-BES DE-FG02-00ER45799. DNB is funded by the Gordon and Betty Moore Foundation's EPiQS Initiative through Grant No. GBMF4533.

K. W. and B. C. contributed equally to this work.

*kwpost@physics.ucsd.edu

[1] M. Hasan and C. Kane, Rev. Mod. Phys. **82**, 3045 (2010).
[2] Y. Xia, D. Qian, D. Hsieh, L. Wray, A. Pal, H. Lin, A. Bansil, D. Grauer, Y. S. Hor, R. J. Cava *et al.*, Nat. Phys. **5**, 398 (2009).
[3] Y. L. Chen, J. G. Analytis, J.-H. Chu, Z. K. Liu, S.-K. Mo, X. L. Qi, H. J. Zhang, D. H. Lu, X. Dai, Z. Fang *et al.*, Science **325**, 178 (2009).

[4] D. Hsieh, Y. Xia, D. Qian, L. Wray, F. Meier, J. Dil, J. Osterwalder, L. Patthey, a. Fedorov, H. Lin *et al.*, Phys. Rev. Lett. **103**, 146401 (2009).
[5] S.-Y. Xu, M. Neupane, C. Liu, D. Zhang, A. Richardella, L. A. Wray, N. Alidoust, M. Leandersson, T. Balasubramanian, J. Sánchez-barriga *et al.*, Nat. Phys. **8**, 616 (2012).
[6] A. Hashibon and C. Elsässer, Phys. Rev. B **84**, 144117 (2011).
[7] B. C. Chapler, K. W. Post, A. R. Richardella, J. S. Lee, J. Tao, N. Samarth, and D. N. Basov, Phys. Rev. B **89**, 235308 (2014).
[8] Y. Jiang, Y. Y. Sun, M. Chen, Y. Wang, Z. Li, C. Song, K. He, L. Wang, X. Chen, Q.-K. Xue *et al.*, Phys. Rev. Lett. **108**, 066809 (2012).
[9] D. Kong, Y. Chen, J. J. Cha, Q. Zhang, J. G. Analytis, K. Lai, Z. Liu, S. S. Hong, K. J. Koski, S.-K. Mo *et al.*, Nat. Nanotechnol. **6**, 705 (2011).
[10] A. A. Reijnders, Y. Tian, L. J. Sandilands, G. Pohl, I. D. Kivlichan, S. Y. F. Zhao, S. Jia, M. E. Charles, R. J. Cava, N. Alidoust *et al.*, Phys. Rev. B **89**, 075138 (2014).
[11] J. Zhang, C.-Z. Chang, Z. Zhang, J. Wen, X. Feng, K. Li, M. Liu, K. He, L. Wang, X. Chen *et al.*, Nat. Commun. **2**, 574 (2011).
[12] L. Wu, M. Brahlek, R. Valdés Aguilar, A. V. Stier, C. M. Morris, Y. Lubashevsky, L. S. Bilbro, N. Bansal, S. Oh, and N. P. Armitage, Nat. Phys. **9**, 410 (2013).
[13] C. S. Tang, B. Xia, X. Zou, S. Chen, H.-W. Ou, L. Wang, a. Rusydi, J.-X. Zhu, and E. E. M. Chia, Sci. Rep. **3**, 3513 (2013).
[14] L. Wu, W.-K. Tse, M. Brahlek, C. Morris, R. Valdés Aguilar, N. Koirala, S. Oh, and N. Armitage, arXiv:1502.04577v1.
[15] It is unclear that optical transitions between SSs and bulk states are theoretically possible due to symmetry and spatial separation, but, moreover, such transitions cannot change the key result (3) relating the SS Drude oscillator strength to the Fermi level.
[16] Z. Li and J. P. Carbotte, Phys. Rev. B **87**, 155416 (2013).
[17] D. N. Basov, R. Averitt, D. van der Marel, M. Dressel, and K. Haule, Rev. Mod. Phys. **83**, 471 (2011).
[18] V. P. Gusynin, S. G. Sharapov, and J. P. Carbotte, Phys. Rev. B **75**, 165407 (2007).
[19] J. Sabio, J. Nilsson, and A. H. Castro Neto, Phys. Rev. B **78**, 075410 (2008).
[20] D. N. Basov, M. M. Fogler, a. Lanzara, F. Wang, and Y. Zhang, Rev. Mod. Phys. **86**, 959 (2014).
[21] See Supplemental Material at http://link.aps.org/supplemental/10.1103/PhysRevLett.115.116804 for details about discussions on optical conductivity in asymmetric bands SS bands, comparing D and n_{SS}, sample growth, the spectroscopic technique and corresponding models of the data, which includes Refs. [14,21–34].
[22] M. Dressel and G. Gruener, *Electrodynamics of Solids: Optical Properties of Electrons in Matter*, 1st ed. (Cambridge University Press, New York, 2002), Vol. 70.
[23] C.-X. Liu, X.-L. Qi, H. J. Zhang, X. Dai, Z. Fang, and S.-C. Zhang, Phys. Rev. B **82**, 045122 (2010).
[24] B. Wunsch, T. Stauber, F. Sols, and F. Guinea, New J. Phys. **8**, 318 (2006).
[25] C. Kittel, *Introduction to Solid State Physics,* 8th ed. (Wiley, New York, 2005).
[26] A. B. Kuzmenko, Rev. Sci. Instrum. **76**, 083108 (2005).
[27] R. D. Averitt and A. J. Taylor, J. Phys. Condens. Matter **14**, R1357 (2002).
[28] R. Yu, W. Zhang, H.-J. Zhang, S.-C. Zhang, X. Dai, and Z. Fang, Science **329**, 61 (2010).
[29] K. W. Post, Y. S. Lee, B. C. Chapler, A. A. Schafgans, M. Novak, A. A. Taskin, K. Segawa, M. D. Goldflam, H. T. Stinson, Y. Ando *et al.*, Phys. Rev. B **91**, 165202 (2015).
[30] R. Valdés Aguilar, A. V. Stier, W. Liu, L. S. Bilbro, D. K. George, N. Bansal, L. Wu, J. Cerne, a. G. Markelz, S. Oh *et al.*, Phys. Rev. Lett. **108**, 087403 (2012).
[31] H. Zhang, C.-X. Liu, X.-L. Qi, X. Dai, Z. Fang, and S.-C. Zhang, Nat. Phys. **5**, 438 (2009).
[32] D. Hsieh, Y. Xia, D. Qian, L. Wray, J. H. Dil, F. Meier, J. Osterwalder, L. Patthey, J. G. Checkelsky, N. P. Ong *et al.*, Nature (London) **460**, 1101 (2009).
[33] M. Neupane, S.-Y. Xu, L. A. Wray, A. Petersen, R. Shankar, N. Alidoust, C. Liu, a. Fedorov, H. Ji, J. M. Allred *et al.*, Phys. Rev. B **85**, 235406 (2012).
[34] T. Arakane, T. Sato, S. Souma, K. Kosaka, K. Nakayama, M. Komatsu, T. Takahashi, Z. Ren, K. Segawa, and Y. Ando, Nat. Commun. **3**, 636 (2012).
[35] M. S. Bahramy, P. D. C. King, A. de la Torre, J. Chang, M. Shi, L. Patthey, G. Balakrishnan, P. Hofmann, R. Arita, N. Nagaosa *et al.*, Nat. Commun. **3**, 1159 (2012).
[36] A. A. Taskin, Z. Ren, S. Sasaki, K. Segawa, and Y. Ando, Phys. Rev. Lett. **107**, 016801 (2011).
[37] V. A. Kulbachinskii, Z. M. Dashevskii, M. Inoue, M. Sasaki, H. Negishi, W. X. Gao, P. Lostak, J. Horak, and A. de Visser, Phys. Rev. B **52**, 10915 (1995).
[38] V. Kulbachinskii, V. Kytin, P. Tarasov, and N. Yuzeeva, Phys. Solid State **52**, 1830 (2010).
[39] L. Fu and C.L. Kane, Phys. Rev. B **76**, 045302 (2007).
[40] I. Garate and L. Glazman, Phys. Rev. B **86**, 035422 (2012).
[41] A. A. Schafgans, K. W. Post, A. A. Taskin, Y. Ando, X.-L. Qi, B. C. Chapler, and D. N. Basov, Phys. Rev. B **85**, 195440 (2012).
[42] W.-K. Tse and A. H. MacDonald, Phys. Rev. Lett. **105**, 057401 (2010).
[43] J. Maciejko, X.-L. Qi, H. D. Drew, and S.-C. Zhang, Phys. Rev. Lett. **105**, 166803 (2010).
[44] Z. Q. Li, E. A. Henriksen, Z. Jiang, Z. Hao, M. C. Martin, P. Kim, H. L. Stormer, and D. N. Basov, Nat. Phys. **4**, 532 (2008).
[45] J. Horng, C.-F. Chen, B. Geng, C. Girit, Y. Zhang, Z. Hao, H. a. Bechtel, M. Martin, A. Zettl, M. F. Crommie *et al.*, Phys. Rev. B **83**, 165113 (2011).
[46] G. S. Jenkins, D. C. Schmadel, A. B. Sushkov, H. D. Drew, M. Bichler, G. Koblmueller, M. Brahlek, N. Bansal, and S. Oh, Phys. Rev. B **87**, 155126 (2013).